The recrystallized grain size piezometer for quartz

Michael Stipp and Jan Tullis

Department of Geological Sciences, Brown University, Providence, Rhode Island, USA

Received 18 August 2003; revised 24 September 2003; accepted 30 September 2003; published 4 November 2003.

[1] In order to determine a recrystallized grain size piezometer for quartz, we deformed Black Hills quartzite in a molten salt assembly in a Griggs apparatus at 1.5 GPa, 800 to 1100°C, and strain rates between $2*10^{-7}$ and $2*10^{-4}$ s^{-1}, conditions which include dislocation creep regimes 2 and 3 of *Hirth and Tullis* [1992]. Flow stresses ranged from 34 ± 16 to 268 ± 38 MPa with corresponding recrystallized grain sizes from 46 ± 15 to 3.2 ± 0.7 μm. The data are well fit by a single piezometer relation, $D = 10^{3.56\pm0.27} * \sigma^{-1.26\pm0.13}$, with no change in slope at the regime 2–3 transition and no effect of temperature or α/β stability field. Another experimental piezometer relation for regime 1 of *Hirth and Tullis* [1992] differs in slope, suggesting that different recrystallization mechanisms require different piezometer calibrations. *INDEX TERMS:* 3902 Mineral Physics: Creep and deformation; 5120 Physical Properties of Rocks: Plasticity, diffusion, and creep; 8030 Structural Geology: Microstructures; 8159 Tectonophysics: Rheology—crust and lithosphere; 8164 Tectonophysics: Stresses—crust and lithosphere. **Citation:** Stipp, M., and J. Tullis, The recrystallized grain size piezometer for quartz, *Geophys. Res. Lett.*, *30*(21), 2088, doi:10.1029/2003GL018444, 2003.

1. Introduction

[2] The ability to infer flow stress magnitudes from the dynamic recrystallization microstructures in naturally deformed rocks requires careful laboratory calibrations. Quartz is a common crustal mineral whose dislocation creep microstructures are sensitive indicators of deformation conditions in the mid to deep crust [e.g., *Dunlap et al.*, 1997; *Stipp et al.*, 2002a]. Recent flow laws [*Luan and Paterson* 1992; *Gleason and Tullis*, 1995; *Hirth et al.*, 2001] give good agreement with natural constraints. However, previously reported recrystallized grain size piezometers for quartz [e.g., *Mercier et al.*, 1977; *Christie et al.*, 1980; *Koch*, 1983] are not reliable, because the experiments had poor stress resolution, in some cases did not achieve steady state, and did not distinguish different mechanisms of dynamic recrystallization. These older piezometers predict unrealistically high flow stresses when extrapolated to natural shear zone conditions [e.g., *Stipp et al.*, 2002b], and most recent studies on natural mylonites have used the theoretical piezometer relation of *Twiss* [1977; Figure 4] to derive flow stresses [e.g., *Dunlap et al.*, 1997].

[3] Three distinct mechanisms of dynamic recrystallization have been distinguished in experimentally deformed quartz aggregates [*Hirth and Tullis*, 1992]; in order of decreasing flow stress these are local grain boundary migration (regime 1 dislocation creep), subgrain rotation (regime 2), and a combination of subgrain rotation and grain boundary migration (regime 3). A similar sequence of recrystallization microstructures is observed in naturally deformed quartz aggregates [e.g., *Dunlap et al.*, 1997; *Stipp et al.*, 2002a]. A difference in the piezometer relation for two distinct recrystallization mechanisms has been found for halite [*Guillopé and Poirier*, 1979] and calcite [*Schmid et al.*, 1980; *Rutter*, 1995]. We wished to determine whether the different recrystallization mechanisms in quartz also have different piezometer relations, and how similar any of them are to the theoretical piezometer of *Twiss* [1977].

2. Methods

[4] Axial compression experiments on Black Hills quartzite (BHQ; grain size ~100 μm) have been carried out in a Griggs apparatus at 1.5 GPa using a molten salt cell (MSC; Figure 1). Cylindrical samples (length = 10 mm, diameter = 5 mm) were weld-sealed in a Pt jacket wrapped in Ni foil. Samples were deformed 'as-is' [water content of ~0.15 wt%; *Post et al.*, 1996]. The top and bottom pistons have a larger diameter (≥6.35 mm) allowing homogeneous sample strain for shortening up to 45% (Figure 1). For the molten salt surrounding the sample, we used 1 bar eutectic mixtures of NaCl/KCl (for 1000 to 1100°C) or LiCl/KCl (for 800 to 900°C); melting points of these mixtures at 1.5 GPa are 900–950°C and ~600°C [*Rybacki et al.*, 1998], respectively. Experimental procedures and data reduction were the same as those of *Gleason and Tullis* [1995].

[5] The externally measured load includes the sample strength, confining pressure and frictional stresses due to the advance of the σ1 piston. We monitor the pressure increase (always <100 MPa) during the experiments and subtract it from the corresponding stress. Four different methods of friction correction were used: (1) inferring friction from additional 'hit' cycles at a faster strain rate before and after the deformation cycle, assuming the increase is linear [*Gleason and Tullis*, 1995]; (2) assuming that friction during the deformation is given by a linear extrapolation of the initial load increase prior to the hit point [*Rybacki et al.*, 1998]; (3) measuring friction directly in experiments with molten salt inside the Pt-jacket; (4) interpolating between two samples with known friction for a sample of intermediate temperature or strain rate. The first method gave the most reproducible results, but the fast hit procedure after the experiment destroys the deformation microstructure. Hence, at several sets of conditions we did a pair of experiments; one was quenched after deformation to provide grain size measurements and one had a fast final hit to provide the friction correction.

0094-8276/03/2003GL018444

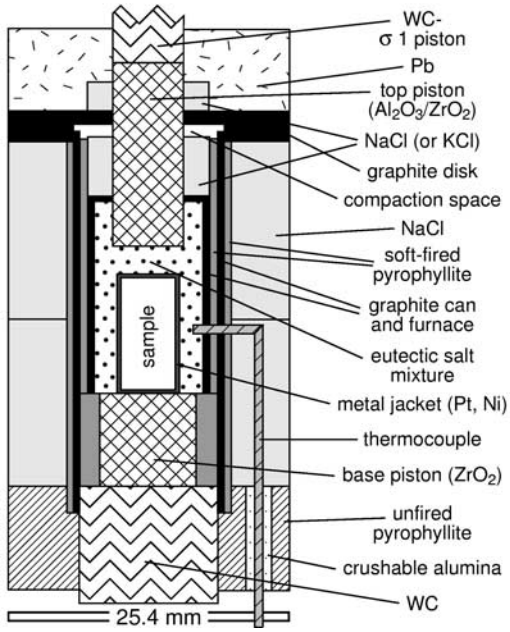

Figure 1. Section through the molten salt cell. See text for further explanation.

[6] Microstructural characterization and grain size measurements were carried out on ultrathin sections (~5–15 μm) using light-optical microscopy. All the deformed samples have an ideal cylindrical shape and a homogeneous microstructure. For sites along the sample center axis parallel to σ1, we used CIP (Computer Integrated Polarization) microscopy [*Panozzo Heilbronner and Pauli*, 1993] to identify and digitize grain boundary outlines. Recrystallized grains were distinguished from porphyroclasts manually and on the basis of the bimodal grain size distribution which occurs in all samples except W-1066 and W-1126. The diameter of each recrystallized grain is defined as the diameter of a circle with the same area, and the average 2-dimensional recrystallized grain size for each sample was calculated as the root mean square diameter from all measured recrystallized grains in that sample. No stereological correction has been applied to the grain size data. The average grain sizes and numbers of measured grains are given in Table 1.

3. Results

[7] Samples were shortened 17 to 46% at temperatures from 800 to 1100°C (Table 1) and constant displacement rates from $1.8*10^{-6}$ mm/s to $1.7*10^{-3}$ mm/s. Recrystallized grain sizes range between 46 ± 15 and 3.2 ± 0.7 μm. Flow stresses were taken as the average over the interval between 10% and the final strain in each experiment, and range between 34 ± 16 and 268 ± 40 MPa (Figure 2, Table 1). The error estimates are based on the maximum stress variation over the steady state range and on the different friction correction methods described above. Our stress resolution is less precise than that of earlier studies, e.g., 5–10 MPa [*Gleason and Tullis*, 1995] or ~5% of the sample strength [*Rybacki et al.*, 1998], because of the high finite strains in our study. For example, the differential stress increase at constant displacement rate can be up to ~11% (for the strain interval from 10–44 %), but in most of our experiments it is <7%.

[8] Based on the data of *Hirth and Tullis*, [1992; their Figure 2a] the deformation conditions of our experiments range from the transition between dislocation creep regimes 1 and 2, up into regime 3, and the light-optical microstructures of our deformed samples confirm this interpretation. At the highest stress, the microstructure consists of inhomogeneously flattened porphyroclasts with patchy extinction and finely sutured grain boundaries along which recrystallized grains occur (Figure 3a). The width of grain boundary bulges is about the same as the diameter of recrystallized grains and the rare subgrains (~3–4 μm). With decreasing differential stress within regime 2, por-

Table 1. Experimental Deformation Conditions and Recrystallized Grain Size Data

sample	temperature [°C]	strain rate [s^{-1}]	axial strain [%]	flow stress [MPa]	recrystallized grain size [μm]	number of grains
W-1126 - β	1100		17		46 ± 15	734
W -1116 - β	1100	$2.1–2.3*10^{-7}$	21	34 ± 16		
W-1066 - β	1100		31		18.0 ± 5.5	676
W-1096 - β	1100	$2.0–2.5*10^{-6}$	32	60 ± 15		
W-1022 - β	1100	$0.8–1.0*10^{-6}$	30	130 ± 30	12.1 ± 3.6	804
W-1029 - β	1100		46		9.0 ± 2.4	876
W-1102 - β	1100	$2.1–2.8*10^{-5}$	33	130 ± 13		
W-1119 - β	1100	$1.8–2.5*10^{-4}$	36	257 ± 35	3.4 ± 0.9	931
W-1025 - β	1050	$1.8–2.4*10^{-6}$	32	87 ± 17	13.6 ± 4.0	476
W-1024 - β	1000		22		11.6 ± 3.2	568
W -1101 - β	1000	$1.8–2.3*10^{-6}$	29	102 ± 9		
W-1051 - β	1000	$1.9–2.9*10^{-5}$	41	189 ± 30	4.6 ± 1.1	638
W-1050 - α	900		34		5.0 ± 1.3	620
W-1099 - α	900	$2.0–2.7*10^{-6}$	33	149 ± 18		
W-1049 - α	900	$1.8–2.8*10^{-5}$	44	268 ± 40	3.2 ± 0.7	777
W-1085 - α	850	$1.9–2.6*10^{-6}$	32	198 ± 30	4.6 ± 1.3	918
W-1030 - α	800	$1.8–2.4*10^{-6}$	32	207 ± 38	4.4 ± 1.1	651
W-739nov-α	700	$\sim 2 * 10^{-6}$	24	368 ± 100	1.9 ± 0.5	706

α and β refer to quartz stability field. Repeated runs for microstructure and mechanical data are listed within the same row. The instantaneous strain rate increase over the interval from 10% to final strain is indicated. The number of recrystallized grains measured in each sample is given. For sample W-739 from *Bishop* [1996] the recrystallized grain size was re-measured. See text for further explanations.

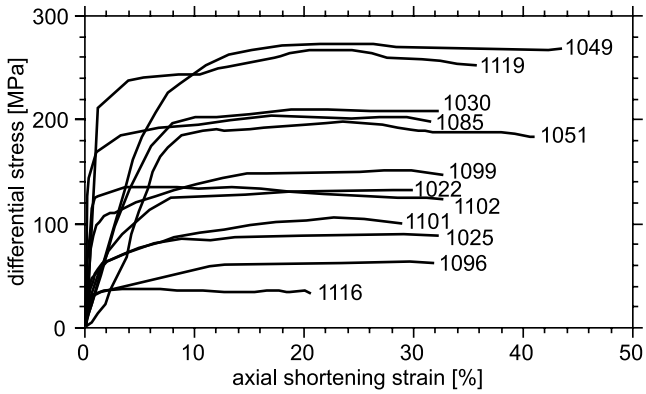

Figure 2. Stress/strain data and sample numbers for the MSC experiments on BHQ; friction corrections are described in the text. Flow stress values in Table 1 are averaged from 10% strain until the end of each run.

phyroclasts are more homogeneously flattened, subgrains are more common, and the amount and size of the recrystallized grains increase. A transition to regime 3 occurs at even lower differential stress, where porphyroclasts are less flattened, their sutured outlines are more irregular, and the amount and size of recrystallized grains increase further (Figure 3b). The width of the sutures is still about the same as the diameter of the recrystallized grains and subgrains. In the sample with the lowest flow stress (34 MPa) it is difficult to differentiate between the porphyroclast remnants and the relatively large (46 μm) recrystallized grains, but the latter are slightly larger than subgrains, indicating a greater contribution of grain boundary migration.

[9] Recrystallized grain size and flow stress data for each BHQ sample deformed in dislocation creep regimes 2 and 3 are plotted in Figure 4. MSC experiments on BHQ for regime 1 dislocation creep were not possible because the high stresses cause corrosion and fracturing of the pistons and mechanical steady state of this coarse-grained material would require very high strain. Thus we have plotted on Figure 4 unpublished data from *Bishop* [1996; presented in *Post and Tullis*, 1999] for dislocation creep regime 1, determined for as-is samples of novaculite (d ≈ 5 μm) deformed in a solid salt assembly at 1.5 GPa, 700° to 850°C and shortening rates of $\sim 2*10^{-6}$ s^{-1} and $2*10^{-5}$ s^{-1}. Steady state flow stresses ranged from 370 ± 100 MPa to 1050 ± 260 MPa; error estimates are inexact due to the uncertainties related to higher friction. Recrystallized grain sizes were measured on SEM images of etched sections by the line intercept method, on transects normal and parallel to σ1; the geometric mean from these two data sets ranges from 2.1 to 1.1 μm. We remeasured one novaculite sample (W-739) with the grain boundary mapping technique on CIP images, and found a recrystallized grain size of 1.9 ± 0.5 μm

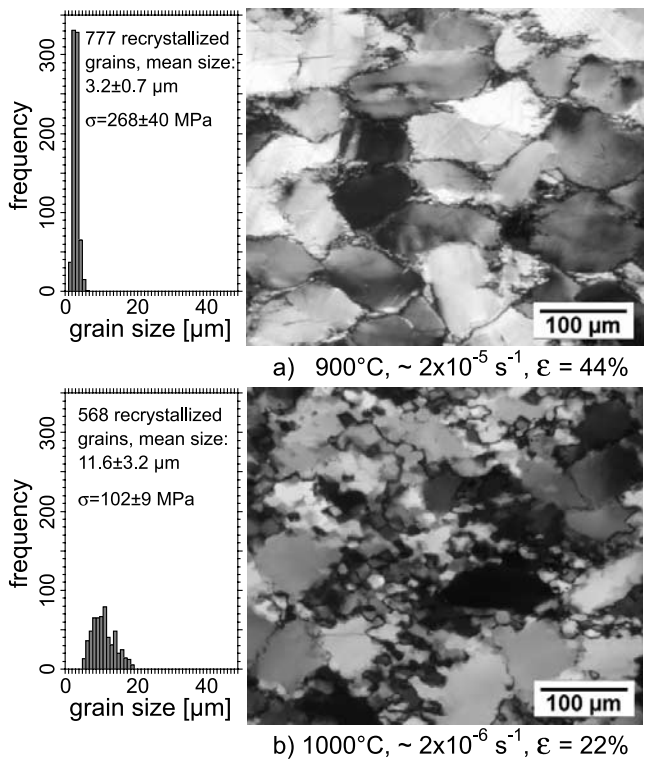

Figure 3. Representative light-optical micrographs (crossed polarizers; shortening direction vertical) and related 2D-recrystallized grain size distributions of deformed BHQ. (a) Porphyroclasts with patchy extinction, bulged grain boundaries and small recrystallized grains (high stress regime 2 close to transition to regime 1; sample W-1049). (b) Porphyroclasts with irregular shape and sutured grain boundaries; suture width and diameter of internal subgrains and surrounding recrystallized grains are about the same (regime 3, sample W-1024). Experimental conditions are indicated.

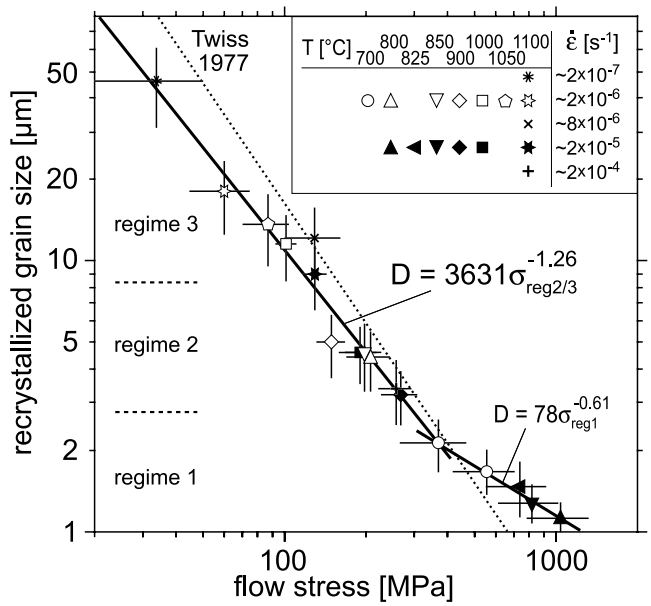

Figure 4. Least squares fit calibrations of a recrystallized grain size piezometer for dislocation creep regime 1 [5 data points, *Bishop*, 1996] and regimes 2 and 3 (11 data points); equations are indicated. Sample W-1126 was not used for calibration due to the different recrystallization microstructure. The theoretical piezometer of *Twiss* [1977] is plotted for comparison using a shear modulus of 42 GPa, a Poisson ratio of 0.15 and a Burgers vector of 5×10^{-4} μm. See text for discussion.

(Table 1) which deviates only slightly from the 2.1 μm measured by *Bishop* [1996].

[10] Considering all of the stress versus recrystallized grain size data together (Figure 4), there appears to be a distinct change in slope between those for regime 1 and regimes 2–3. A single piezometer relation was fit to all the data for regimes 2 and 3, with the exception of the lowest stress sample (W-1116/W-1126); a least squares fit results in the relation: $D = 10^{3.56\pm0.27} * \sigma^{-1.26\pm0.13}$. For the regime 1 novaculite data, the piezometer is: $D = 10^{1.89\pm0.11} * \sigma^{-0.61\pm0.04}$. We believe that a separate piezometer relation for regime 1 is warranted, based on the distinct microstructural and mechanical changes at the regime 1–2 transition [*Hirth and Tullis*, 1992]. However, the regime 2–3 transition does not show a significant change in piezometer slope, perhaps indicating that there is not a fundamental change in recrystallization mechanism. The lowest stress sample has a good fit to the regime 2–3 piezometer (Figure 4), but was excluded from the calibration because its microstructure deviates from the other regime 3 microstructures and does not allow a clear distinction between porphyroclasts and recrystallized grains.

4. Discussion

[11] The lack of a piezometer change between regimes 2 and 3 may indicate that the microstructural changes described by *Hirth and Tullis* [1992] are mechanically insignificant and/or do not correspond to a major transition in recrystallization mechanism. *Hirth and Tullis* [1992] define the transition to regime 3 as occurring when recrystallized grains become larger than subgrains, due to increased grain boundary mobility. Their distinction was made on the basis of transmission electron microscope (TEM) observations whereas we have used light-optical criteria, and it is well known that light-optical subgrains are larger than coexisting TEM-scale subgrains [e.g., *White*, 1979]. Over our experimental range from 268 to 60 MPa, we observe that recrystallized grains (3.2 to 18 μm) have the same size as subgrains, and only in the sample deformed at 34 MPa are the recrystallized grains (~46 μm) larger than coexisting subgrains. Further experiments at even lower stresses are required to determine whether a different piezometer relation is necessary to fit data for this different recrystallization microstructure. Interestingly, *Stipp et al.* [2002b] found a marked change in slope of recrystallized grain size versus temperature between 24 and 58 μm, correlating with a major difference in the recrystallization microstructure, which strongly suggests a different piezometer relation for stresses just below the current experimental range.

[12] The slope change between the regime 1 data of *Bishop* [1996] and our regime 2–3 data (Figure 4) could be due to a change in the dominant recrystallization mechanism; *Hirth and Tullis* [1992] observed subgrain formation in regime 2 but not in regime 1. Such a slope change for regime 1 cannot be tested on the present database of natural quartz mylonites. The steeper slope for regime 1, however, is similar to that for the only other study of this high stress recrystallization mechanism, in feldspar aggregates [*Post and Tullis*, 1999]. Alternatively, the steeper slope for the regime 1 data might result from inadequate friction corrections in the solid confining medium experiments.

[13] There is no independent temperature effect on the recrystallized grain size of quartz, within the uncertainty of our data (Figure 4); samples with a similar flow stress but different temperatures have very similar recrystallized grain sizes. The α/β-quartz transition also has no effect on the recrystallized grain size piezometer, consistent with previous findings that it has no effect on the flow law [*Gleason and Tullis*, 1995] or the lattice preferred orientations in experimentally deformed quartz aggregates [*Gleason et al.*, 1993].

[14] The theoretical piezometer of *Twiss* [1977; Figure 4], which has been widely used for flow stress determinations in naturally deformed rocks despite being critized for an incorrect application of equilibrium thermodynamics [e.g., *De Bresser et al.*, 2001], is close to our regime 2–3 piezometer. At present our experimental calibration can be applied to dynamically recrystallized quartz rocks with grain sizes of ~3–45 μm, but it remains to be determined whether larger and smaller recrystallized grain sizes require a different piezometer relation.

[15] **Acknowledgments.** Supported by Swiss NF research comm. Basel 81RS-63210 US NSF EAR-0106850 and 0208150 and a Novartis stipendium to MS. We are grateful to R. Yund and C. Holyoke for many contributions to this research; we also thank E. Rybacki, D. Goldsby, R. Heilbronner, H. Stünitz and G. Hirth for helpful discussions. Thorough reviews by H. de Bresser and an anonymous reviewer are gratefully acknowledged.

References

Bishop, R. R., Grain boundary migration in experimentally deformed quartz aggregates: The relationship between dynamically recrystallized grain size and steady state flow stress, *B. Sc. thesis*, 36 pp., Brown Univ., 1996.

Christie, J. M., A. Ord, and P. S. Koch, Relationship between recrystallized grain size and flow stress in experimentally deformed quartzite, *Eos Trans. AGU*, *61*, 377, 1980.

De Bresser, J. H. P., J. H. Ter Heege, and C. H. Spiers, Grain size reduction by dynamic recrystallization: Can it result in major rheological weakening?, *Intern. J. Earth Sc.*, *90*, 28–45, 2001.

Dunlap, W. J., G. Hirth, and C. Teyssier, Thermomechanical evolution of a ductile duplex, *Tectonics*, *16*, 983–1000, 1997.

Gleason, G. C., and J. Tullis, A flow law for dislocation creep of quartz aggregates determined with the molten salt cell, *Tectonophysics*, *247*, 1–23, 1995.

Gleason, G. C., J. Tullis, and F. Heidelbach, The role of dynamic recrystallization in the development of lattice preferred orientations in experimentally deformed quartz aggregates, *J. Struct. Geol.*, *15*, 1145–1168, 1993.

Guillopé, M., and J. P. Poirier, Dynamic recrystallization during creep of single-crystalline halite: An experimental study, *J. Geophys. Res.*, *84*, 5557–5567, 1979.

Hirth, G., C. Teyssier, and W. J. Dunlap, An evaluation of quartzite flow laws based on comparisons between experimentally and naturally deformed rocks, *Intern. J. Earth Sc.*, *90*, 77–87, 2001.

Hirth, G., and J. Tullis, Dislocation creep regimes in quartz aggregates, *J. Struct. Geol.*, *14*, 145–159, 1992.

Koch, P. S., Rheology and microstructures of experimentally deformed quartz aggregates, Ph.D. thesis, 464 pp., Univ. of California, Los Angeles, 1983.

Luan, F. C., and M. S. Paterson, Preparation and deformation of synthetic aggregates of quartz, *J. Geophys. Res.*, *97*, 301–320, 1992.

Mercier, J.-C. C., D. A. Anderson, and N. L. Carter, Stress in the lithosphere: Inferences from steady state flow of rocks, *Pageoph.*, *115*, 199–226, 1977.

Panozzo Heilbronner, R., and C. Pauli, Integrated spatial and orientation analysis of quartz c-axes by computer-aided microscopy, *J. Struct. Geol.*, *15*, 369–382, 1993.

Post, A., and J. Tullis, A recrystallized grain size paleopiezometer for experimentally deformed feldspar aggregates, *Tectonophysics*, *303*, 159–173, 1999.

Post, A. D., J. Tullis, and A. Yund, Effects of chemical environment on dislocation creep of quartzite, *J. Geophys. Res.*, *101*, 22,143–22,155, 1996.

Rutter, E. H., Experimental study of the influence of stress, temperature, and strain on the dynamic recrystallization of Carrara marble, *J. Geophys. Res.*, *100*, 24,651–24,663, 1995.

Rybacki, E., J. Renner, K. Konrad, W. Harbott, F. Rummel, and B. Stöckhert, A servohydraulically-controlled deformation apparatus for rock deformation under conditions of ultra-high pressure metamorphism, *Pageoph.*, *152*, 579–606, 1998.

Schmid, S. M., M. S. Paterson, and J. N. Boland, High temperature flow and dynamic recrystallization in Carrara marble, *Tectonophysics*, *65*, 245–280, 1980.

Stipp, M., H. Stünitz, R. Heilbronner, and S. M. Schmid, Dynamic recrystallization of quartz: Correlation between natural and experimental conditions, *Geol. Soc. Spec. Publ. London*, *200*, 171–190, edited by S. De Meer, M. R. Drury, J. H. P. De Bresser, and G. M. Pennock, 2002a.

Stipp, M., H. Stünitz, R. Heilbronner, and S. M. Schmid, The eastern Tonale fault zone: A "natural laboratory" for crystal plastic deformation of quartz over a temperature range from 250°C to 700°C, *J. Struct. Geol.*, *24*, 1861–1884, 2002b.

Twiss, R. J., Theory and applicability of a recrystallized grain size paleopiezometer, *Pageoph.*, *115*, 227–244, 1977.

White, S. H., Difficulties associated with paleo-stress estimates, *Bull. Minéral.*, *102*, 210–215, 1979.

M. Stipp and J. Tullis, Brown Univ., P.O. Box 1846, Providence RI 02912, USA. (michael_stipp@brown.edu)